# Contrasting anatomical and biochemical controls on mesophyll conductance across plant functional types

Jürgen Knauer, Matthias Cuntz, John R Evans, Ülo Niinemets, Tiina Tosens, Linda-liisa Veromann-jürgenson, Christiane Werner, Sönke Zaehle

New Phytologist

Research

# Contrasting anatomical and biochemical controls on mesophyll conductance across plant functional types

**Jürgen Knauer[1,2,3], Matthias Cuntz[4], John R. Evans[5], Ülo Niinemets[6], Tiina Tosens[6], Linda-Liisa Veromann-Jürgenson[6], Christiane Werner[7] and Sönke Zaehle[3]**

[1]Hawkesbury Institute for the Environment, Western Sydney University, Penrith, NSW 2751, Australia; [2]Climate Science Centre, CSIRO Oceans and Atmosphere, Canberra, ACT 2601, Australia; [3]Max Planck Institute for Biogeochemistry, 07745 Jena, Germany; [4]AgroParisTech, UMR Silva, INRAE, Université de Lorraine, 54000 Nancy, France; [5]ARC Centre of Excellence for Translational Photosynthesis, Research School of Biology, The Australian National University, Canberra, ACT 2601, Australia; [6]Institute of Agricultural and Environmental Sciences, Estonian University of Life Sciences, 51006 Tartu, Estonia; [7]Ecosystem Physiology, University of Freiburg, 79110 Freiburg, Germany

Author for correspondence:
*Jürgen Knauer*
*Email: j.knauer@westernsydney.edu.au*

Received: *16 March 2022*
Accepted: *30 June 2022*

*New Phytologist* (2022) **236:** 357–368
**doi**: 10.1111/nph.18363

**Key words:** leaf anatomy, leaf internal $CO_2$ transfer, leaf gas exchange, leaf nutrient content, photosynthetic capacity, photosynthetic limitation.

## Summary

- Mesophyll conductance ($g_m$) limits photosynthesis by restricting $CO_2$ diffusion between the substomatal cavities and chloroplasts. Although it is known that $g_m$ is determined by both leaf anatomical and biochemical traits, their relative contribution across plant functional types (PFTs) is still unclear.
- We compiled a dataset of $g_m$ measurements and concomitant leaf traits in unstressed plants comprising 563 studies and 617 species from all major PFTs. We investigated to what extent $g_m$ limits photosynthesis across PFTs, how $g_m$ relates to structural, anatomical, biochemical, and physiological leaf properties, and whether these relationships differ among PFTs.
- We found that $g_m$ imposes a significant limitation to photosynthesis in all $C_3$ PFTs, ranging from 10–30% in most herbaceous annuals to 25–50% in woody evergreens. Anatomical leaf traits explained a significant proportion of the variation in $g_m$ ($R^2 > 0.3$) in all PFTs except annual herbs, in which $g_m$ is more strongly related to biochemical factors associated with leaf nitrogen and potassium content.
- Our results underline the need to elucidate mechanisms underlying the global variability of $g_m$. We emphasise the underestimated potential of $g_m$ for improving photosynthesis in crops and identify modifications in leaf biochemistry as the most promising pathway for increasing $g_m$ in these species.

## Introduction

The supply of $CO_2$ to the photosynthetic machinery depends on how efficiently it can be transferred from the ambient air to the chloroplasts located inside the leaf mesophyll cells. This efficiency can be quantified as a series of resistances (or the inverse quantity, conductances) caused by the leaf boundary layer, the stomata, as well as leaf internal components in the mesophyll. This last part of the $CO_2$ pathway, the mesophyll conductance ($g_m$), accounts for one-third to one-half of the overall $CO_2$ drawdown from the atmosphere to the chloroplasts (Warren, 2008; Flexas *et al.*, 2012) and therefore constitutes a major controlling factor of the $CO_2$ concentration available for photosynthesis. Knowledge of the determinants of $g_m$ can therefore support efforts aiming to improve photosynthesis to ensure that global food and bioenergy demand can be met in the future (von Caemmerer & Evans, 2010; Ort *et al.*, 2015). Furthermore, information of how $g_m$ is related to key leaf structural and biochemical traits is important for understanding and modelling carbon uptake from the leaf to the global scale (Niinemets *et al.*, 2009; Sun *et al.*, 2014; Knauer *et al.*, 2019, 2020).

The pathway of $CO_2$ within plant leaves can be divided into several components, which in combination determine the magnitude of $g_m$: the intercellular airspaces, the cell wall, the plasma membrane, the cytosol, the chloroplast envelope, and the chloroplast stroma (Niinemets & Reichstein, 2003; Evans *et al.*, 2009). Some of the conductances within these components depend primarily on biophysical characteristics (e.g. surface area of chloroplasts exposed to intercellular airspaces, cell wall thickness and porosity) and are therefore subject to anatomical constraints, whereas $CO_2$ transfer through other cell compartments such as membranes and the cytosol are primarily the result of biochemical factors, in particular the expression of proteins associated with $CO_2$ transfer. These include aquaporins (cooporins), proteins that regulate water and $CO_2$ transfer across membranes (Uehlein *et al.*, 2003), and carbonic anhydrase (CA), which governs the interconversion between $CO_2$ and bicarbonate in the cytosol and chloroplast stroma (Fabre *et al.*, 2007; Evans *et al.*, 2009). Despite the fact that it is well established that $g_m$ is affected by both anatomical and biochemical leaf traits (Warren, 2008; Flexas *et al.*, 2012, 2018; Gago *et al.*, 2020), their relative contribution across plant functional types (PFTs) has not yet been assessed.

The complexity of the $CO_2$ diffusion pathway within leaves results in considerable uncertainties regarding the contributions of the individual components to the overall conductance as well as the associated importance of key anatomical and biochemical traits. One possible avenue to elucidate the role of certain leaf traits in determining $g_m$ are gas diffusion models that calculate the component conductances based on biophysical and biochemical principles (Niinemets & Reichstein, 2003; Tomás *et al.*, 2013; Berghuijs *et al.*, 2015; Xiao & Zhu, 2017). However, these models either do not take all relevant mechanisms into account (e.g. biochemistry, location of individual elements of the diffusion pathway) or require parameters that are unknown or only available for a few species, which hinders the interpretation of these models as well as their application across PFTs.

An alternative approach followed by many studies is to use correlation analysis to investigate to what extent $g_m$ measurements are related to leaf anatomical and biochemical traits. However, most studies are restricted to one or a few species of the same PFT and are subject to differences in growth environments, measurement conditions, as well as assumptions and uncertainties inherent in different measurement approaches (Pons *et al.*, 2009). These differences can hamper a direct comparison between individual studies and preclude robust conclusions. In addition, correlations can only provide associative rather than causal relationships between $g_m$ and leaf traits. Despite these limitations, a correlative approach can provide information about key traits covarying with $g_m$ and therefore highlight the trait syndromes responsible for the variation in $g_m$, especially if relationships emerge across studies, species, and conditions (e.g. Xiong & Flexas, 2018; Ren *et al.*, 2019; Elferjani *et al.*, 2021).

Here, we present the hitherto largest published dataset of $g_m$ measurements compiled from the literature (comprising 563 studies). We performed a comprehensive analysis that aimed to investigate the relationships between $g_m$ and accompanying leaf structural, anatomical, biochemical and physiological traits measured on the same set of plants. The overarching goal of this top-down approach was to identify patterns between $g_m$ and leaf traits that are robust with respect to existing confounding effects of different species and genotypes, growth conditions, or methodological considerations, and that may guide future research priorities. In particular, we asked (1) how much $g_m$ limits photosynthesis across PFTs, (2) to what extent leaf anatomical and biochemical factors can explain variations in $g_m$ across and within PFTs, and (3) how our findings could be used to enhance $g_m$ and photosynthesis.

## Materials and Methods

### Literature review

A literature review was conducted in Google Scholar using the search terms 'mesophyll conductance' and 'leaf internal conductance'. All peer-reviewed studies that were published online until 31 December 2020 were considered. Criteria for inclusion into the dataset were that $g_m$ was estimated at leaf level using any published method and that it was defined according to Fick's first law as $g_m = A_n/(C_i - C_c)$, where $A_n$ is net photosynthesis, $C_i$ is the intercellular $CO_2$ concentration, and $C_c$ is the chloroplastic $CO_2$ concentration. No modelled $g_m$ data were included. $g_m$ values and all accompanying traits presented here were extracted from tables or the text, if possible, otherwise digitised from figures using PlotDigitizer v.2.6.8 (http://plotdigitizer.sourceforge.net/). The compilation aimed to represent unstressed, young, but fully expanded and high light-adapted leaves, albeit these criteria were not always explicitly stated. In studies including treatments, only data from the control treatment were extracted. Only one (aggregated) $g_m$ value per set of plants was included in the dataset.

### Data processing

**Mesophyll conductance** Mesophyll conductance values were standardised to represent $g_m$ to $CO_2$ transfer in units of mol $m^{-2}$ $s^{-1}$. Values reported in liquid-phase equivalent units (mol $m^{-2}$ $s^{-1}$ $bar^{-1}$ or μmol $m^{-2}$ $s^{-1}$ $Pa^{-1}$) were standardised to an atmospheric pressure of 100 kPa (=1 bar) if either the atmospheric pressure or the elevation (from which mean atmospheric pressure was derived) were reported, otherwise an atmospheric pressure of 100 kPa was assumed. Measurements not performed at 25°C or not standardised to 25°C in the original studies were standardised to 25°C (denoted as $g_{m,25}$) using the temperature response of Bernacchi *et al.* (2002) measured for *Nicotiana tabacum*. The functional shape of this temperature function was confirmed by an independent study over a wide temperature range (Evans & von Caemmerer, 2013). To characterise the degree of uncertainty associated with the temperature response of $g_m$, the analysis was also performed using a weaker temperature response derived for *Arabidopsis thaliana* (Walker *et al.*, 2013). Values at the original measurement temperature (denoted as $g_m$) were retained in the dataset and reported here if shown together with other physiological measurements conducted at the same temperature.

Measurements were discarded if they met one or more of the following criteria: (1) measurement temperature lower than 15°C or higher than 35°C, or not reported; (2) measurement irradiance lower than 300 μmol $m^{-2}$ $s^{-1}$; (3) measurement $CO_2$ concentration lower than 300 μmol $mol^{-1}$ or higher than 500 μmol $mol^{-1}$; (4) measurements associated with unrealistic $CO_2$ drawdown values according to Fick's first law ($C_i - C_c = A_n/g_m$ greater than 300 μmol $mol^{-1}$ or smaller than 10 μmol $mol^{-1}$); and (5) values identified as outliers. Outliers were detected with a two-step procedure: first, extreme values exceeding 2 mol $m^{-2}$ $s^{-1}$ or 1 mol $m^{-2}$ $s^{-1}$ for herbaceous and woody plants, respectively, were excluded. Second, the remaining data were log-transformed and all data lower than the first quartile minus 1.5 times the interquartile range (IQR) and higher than the third quartile plus 1.5 times the IQR were excluded. Step two was performed separately for each PFT. Sixty-one outliers were detected across the dataset. In total, data filtering led to the exclusion of 200 datapoints that left 1683 data points (89.4%) from 492 studies (87.4%) for subsequent analysis.

All published methods for estimating $g_m$ were considered for the analysis (Supporting Information Fig. S1). If $g_m$ was

measured with both the curve fitting and a second method, only the second method was used for the analysis. If $g_m$ was measured with two methods other than curve fitting, $g_m$ was calculated as the mean of the two methods. The associated averaging of $g_m$ measurements across methods decreased the available data by another 244 data points.

Species were grouped into the following major PFTs according to their evolutionary lineage and growth habits (leaf longevity): ferns, evergreen gymnosperms, woody evergreen angiosperms, woody deciduous angiosperms, $C_3$ perennial herbaceous, $C_3$ annual and biennial herbaceous (from this point forwards $C_3$ annual herbaceous), in which herbaceous includes both forbs and grasses. The dataset also contains values for Crassulacean acid metabolism (CAM) plants, $C_4$ plants (both annual and perennial herbaceous), semideciduous angiosperms, deciduous gymnosperms, as well as fern allies and mosses, but these PFTs (in total 102 data points (7.1%) after data filtering) were not included in this analysis due to limited data availability. Excluding these PFTs from the dataset left 1337 out of 1883 datapoints (71.0%) from 476 studies (84.5%) and 495 species (80.2%) available for analysis in this study.

**Accompanying traits and variables** In addition to $g_m$, leaf physiological, structural, anatomical and biochemical traits and variables, as well as ancillary information such as measurement method, measurement and growth conditions, plant age, etc. were extracted from the studies (please refer to Table S1 for a full list and the full dataset (Knauer *et al.*, 2022) for additional traits and variables not presented here). All observations for a given trait were converted to a common unit as specified in Table S1. Care was taken that all extracted values were measured in the same experiments and treatments as the presented $g_m$ values. That means that all traits analysed here were measured in the same set of plants subject to the same experimental treatment, growth conditions and measurement conditions.

**Photosynthetic limitation** Relative photosynthetic limitation caused by $g_m$ ($L_m$) was originally proposed by Farquhar & Sharkey (1982) for stomatal conductance ($g_s$) and subsequently applied to $g_m$ (Epron *et al.*, 1995; Warren *et al.*, 2003):

$$L_m = \frac{A_{np} - A_n}{A_{np}} \times 100 \qquad \text{Eqn 1}$$

where $A_n$ is the light-saturated net photosynthesis measured at ambient $CO_2$ concentration (i.e. assuming $g_m$ and $g_s$ as measured), and $A_{np}$ is the net photosynthesis at $C_c = C_i$ (i.e. assuming infinite $g_m$ and $g_s$ as measured). As most studies did not report all parameters needed to calculate $L_m$, data analysed here were limited to those directly reported in the studies. $L_m$ as defined in Eqn 1 was preferred over the limitation analysis suggested by Grassi & Magnani (2005) because it allows inferences on the absolute limitation of $A_n$ by $g_m$, whereas the method by Grassi & Magnani (2005) quantifies the photosynthetic limitation of $g_m$ relative to those imposed by $g_s$ and photosynthetic capacity.

### Statistical analysis

Pairwise relationships between $g_m$ and leaf traits were characterised with robust linear or robust nonlinear regressions using the ROBUSTBASE R package (Maechler *et al.*, 2022). Differences in the median among groups was tested with Dunn's test of multiple comparisons, using the *dunnTest* function in the R package FSA (Ogle *et al.*, 2022). Statistical significance ($P < 0.05$) of the relationships was only tested and reported if the number of measurements were ≥ 12, unless stated otherwise.

As $g_m$ data show a gamma distribution rather than a normal distribution, linear regression models are not ideal for modelling $g_m$. Therefore, to predict $g_m$ from anatomical traits we applied a generalised linear model (glm) with a gamma error distribution and a log-link function. To assess glm model fits, McFadden's pseudo $R^2$ was calculated as $R^2 = 1 - \frac{\ln L(M_{Full})}{\ln L(M_{Null})}$, where ln $L(M_{full})$ is the log-likelihood of the full model (i.e. all coefficients fitted) and ln $L(M_{Null})$ is the log-likelihood of the null model (i.e. only intercept fitted). All data processing and statistical analysis was conducted in R v.4.1.2 (R Core Team, 2021).

## Results

After data filtering 1337 individual $g_m$ values from 476 studies representing all published methods on estimating $g_m$ were left for analysis (please refer to Fig. S1 for the number of studies per year and method used for estimating $g_m$). The data show typical relationships between $g_m$ and other leaf gas exchange variables (Fig. 1). We found moderate correlations between $g_m$ and light-saturated net photosynthesis ($A_n$) and to a lesser extent also between $g_m$ and stomatal conductance to $CO_2$ ($g_{s,c}$). Generally, a stronger relationship was observed for herbaceous plants and deciduous angiosperms compared with woody species for both $A_n$ and $g_{s,c}$ (Fig. 1a,b). $g_m$ does not show a clear relationship with the ratio of intercellular $CO_2$ concentration ($C_i$) to ambient $CO_2$ concentration ($C_a$) but a positive relationship with the chloroplastic $CO_2$ concentration ($C_c$) and the $C_c : C_a$ ratio. There is furthermore a clear inverse relationship between $g_m$ and the $CO_2$ drawdown ($C_i - C_c$) across PFTs, in which herbaceous annuals tend to show the highest $CO_2$ drawdown for a given $g_m$ (Fig. 1f).

Mesophyll conductance standardised to 25°C ($g_{m,25}$, please refer to the Materials and Methods section) is higher in herbaceous species than in woody species and higher in species with annual leaves compared with those with long-lived leaves in both herbaceous and woody plants. Ferns showed the lowest $g_m$ values of all PFTs (Fig. 2a). Absolute values of $g_{m,25}$ depend on the standardisation function used, which also affects statistical relationships found here (please refer to Table S2). However, differences were mostly minor or limited to individual PFTs and therefore did not affect key results. We also tested whether different measurement methods (fluorescence, isotope, curve fitting and others (please refer to e.g. Pons *et al.*, 2009 for an overview of the different methods)) predict different magnitudes of $g_m$. While we find differences among methods for some PFTs and a general tendency of the isotope method to yield higher values

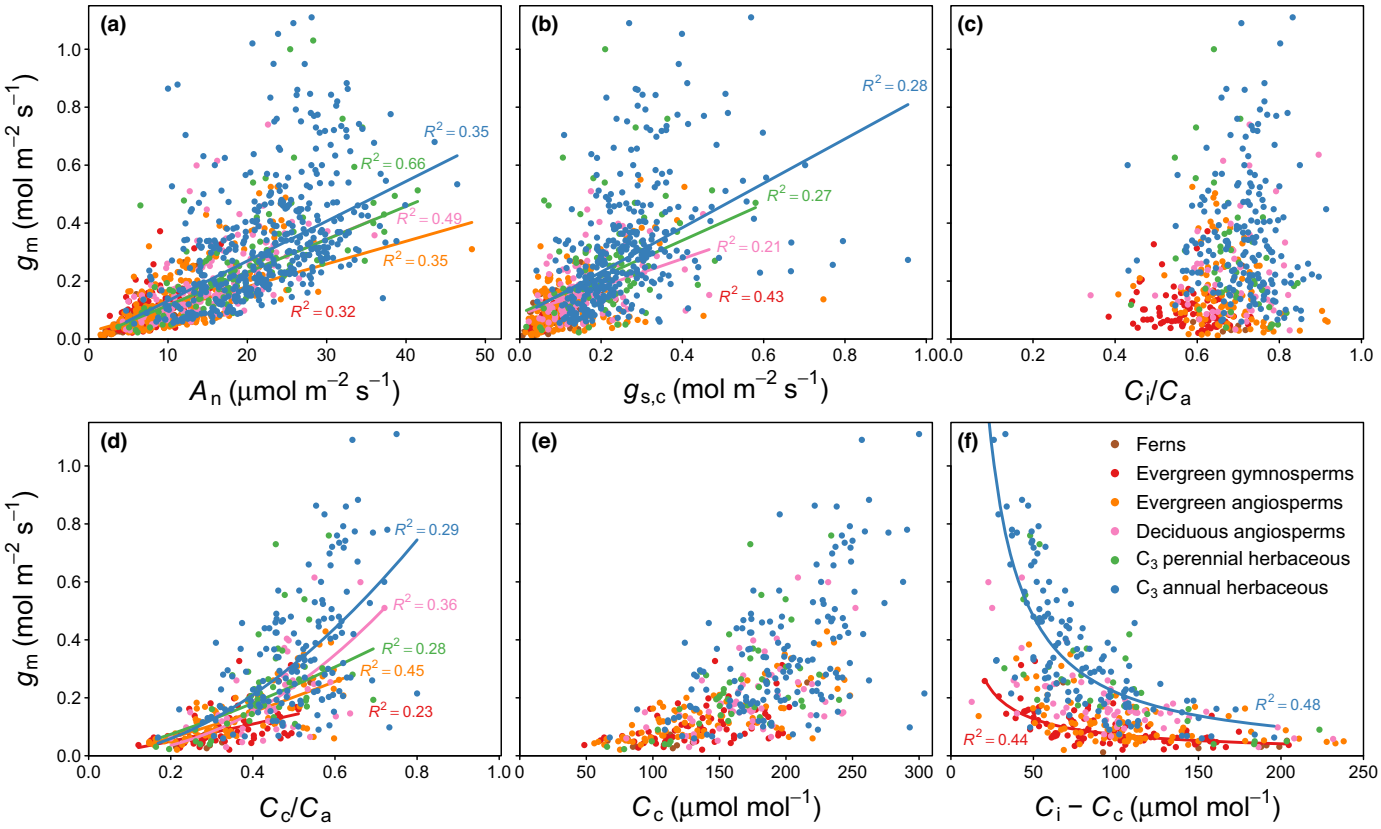


**Fig. 1** Relationship between mesophyll conductance ($g_m$) and leaf gas exchange variables: (a) net photosynthesis ($A_n$), (b) stomatal conductance to $CO_2$ ($g_{s,c}$), (c) the ratio of intercellular $CO_2$ concentration ($C_i$) to ambient $CO_2$ concentration ($C_a$), (d) the ratio of chloroplastic $CO_2$ concentration ($C_c$) to $C_a$, (e) $C_c$, and (f) the $CO_2$ drawdown between intercellular airspaces and the chloroplast stroma ($C_i - C_c$). Robust linear regression was applied in panels (a, b) and robust nonlinear regression of the form $y = ax^b$ in all other panels. Model fits and corresponding $R^2$ values are displayed if the model $P$-value < 0.05.

compared with the fluorescence and curve fitting method, statistically significant differences among methods could only be detected for some PFTs (Fig. S2).

We investigated to what extent the measured values of $g_m$ limit photosynthesis (Fig. 2b). We compiled data representing the relative limitation of $A_n$ by $g_m$ ($L_m$; Eqn 1) (Farquhar & Sharkey, 1982; Epron *et al.*, 1995), a metric quantifying to what extent $A_n$ could be enhanced if $g_m$ was infinitely high (please refer to the Materials and Methods section). We found that at ambient $CO_2$ concentrations $g_m$ imposes a significant limitation to photosynthesis in most plants (Fig. 2b). $L_m$ increases sharply with decreasing $g_m$ and reaches 35–55% if $g_m$ is smaller than 0.1 mol m$^{-2}$ s$^{-1}$. At the higher end of the $g_m$ range $L_m$ approaches 0. Using the 95% confidence interval of the fitted function in Fig. 2(b) to predict $L_m$ from a typical range (25$^{th}$ to 75$^{th}$ quantile) of measured $g_m$ values as shown in Fig. 2(a) suggests that the limitation of photosynthesis by $g_m$ amounts to 29–49% in evergreen gymnosperms, 23–47% in evergreen angiosperms, and 20–40% in deciduous angiosperms for representative plants in each PFT (i.e. those with $g_m$ in the interquartile range; Fig. 2a). Individual $L_m$ values may be well above or below the PFT-specific averages (Fig. 2b) and the ranges of $L_m$ across PFTs overlap to a large extent, reflecting the large spread of $g_m$ values within PFTs (Fig. 2a). In addition, as $L_m$ depends not only on the absolute value of $g_m$ but also on $g_s$ and leaf photosynthetic capacity (foremost the maximum carboxylation rate ($V_{cmax}$)), interspecific variations in these two variables are likely to contribute to the scatter in Fig. 2(b) (please refer to e.g. fig. 1 in Epron *et al.*, 1995). $L_m$ is lower in herbaceous plants but still amounted to 16–35% and 9–32% in representative perennial and annual herbs, respectively. Notably, photosynthetic limitations of < 10% are typically only present if $g_m$ exceeds *c.* 0.5 mol m$^{-2}$ s$^{-1}$, a value that is commonly not reached even in annual herbaceous plants, which include most crops (Figs 2a, S3). The fitted function in Fig. 2(b) suggests a limitation of 20.9% (95% confidence interval = (17.6, 24.2)%) for an average crop species (median $g_{m,25}$ = 0.26 mol m$^{-2}$ s$^{-1}$, Fig. S3) and higher values in species with low $g_{m,25}$ such as rice (*Oryza sativa*; 0.23 mol m$^{-2}$ s$^{-1}$) and bean (*Phaseolus vulgaris*; 0.24 mol m$^{-2}$ s$^{-1}$).

We next analysed which leaf traits determine absolute values of $g_m$. We did not find significant relationships between the magnitude of $g_m$ and commonly measured leaf structural traits. Leaf dry mass per area (LMA), leaf thickness, mesophyll thickness, leaf density, and leaf porosity were not related to $g_m$ neither across nor within PFTs (Fig. S4). Stomatal characteristics (stomatal

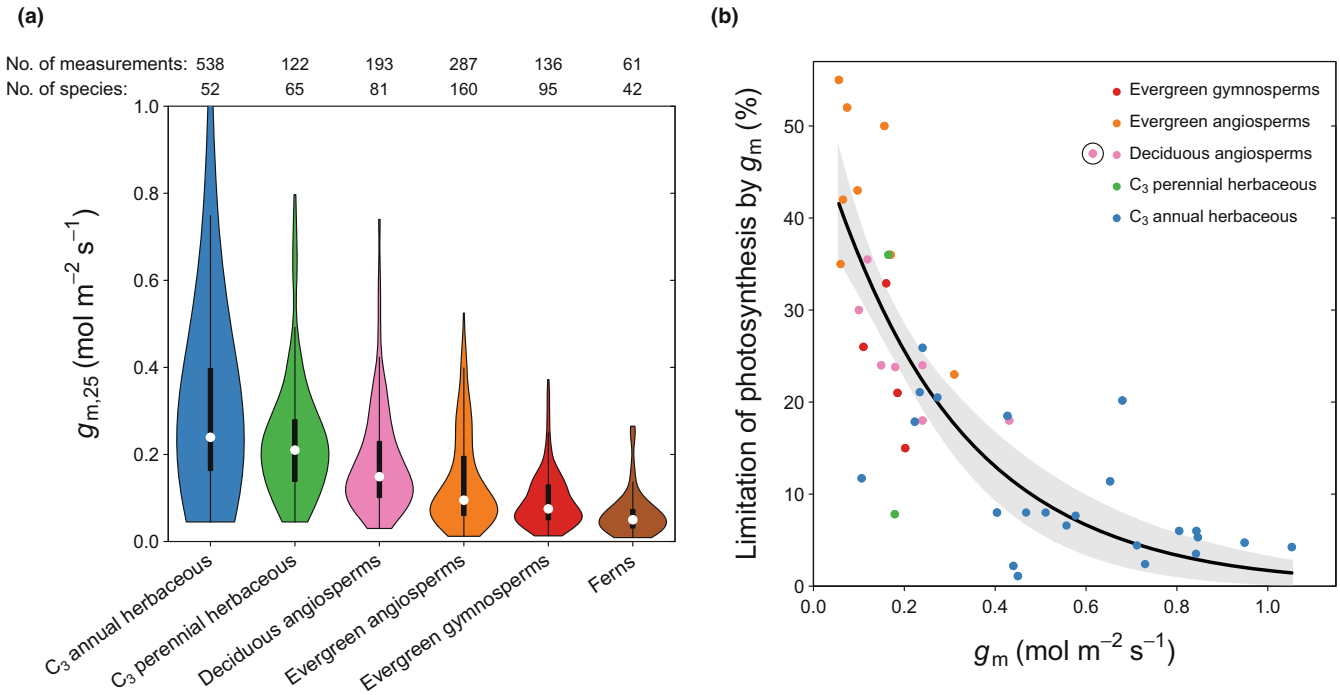


**Fig. 2** (a) Violin plots showing the distribution of mesophyll conductance measurements standardised to 25°C ($g_{m,25}$) for main plant functional types (PFTs). Dots represent group medians, black bars represent the interquartile range, and black lines represent 1.5 times the interquartile range. All PFT medians were statistically significant from each other according to Dunn's test. (b) Limitation of leaf photosynthesis by $g_m$ across plant functional types. Photosynthetic limitation ($L_m$) was calculated as $(A_{np} - A_n)/A_{np} \times 100$ (Eqn 1), where $A_n$ is measured net photosynthesis and $A_{np}$ is net photosynthesis assuming $C_i = C_c$ (please refer to the Materials and Methods section). The fitted line represents the nonlinear regression $L_m = 50.2 \exp(-3.37\, g_m)$ ($R^2 = 0.70$, $P < 0.001$). The circled point (*Prunus persica*) was excluded from the regression. The shaded area represents the 95% confidence interval of the regression fit.

density, area, and length) were in general unrelated to $g_m$ but $g_m$ in annual herbaceous plants showed a significant ($P < 0.05$) decrease with stomatal length and area, and a significant increase with stomatal density, although correlations were generally weak (Fig. S4).

Two anatomical traits were found to play a significant role for $g_m$ across PFTs: chloroplast surface area exposed to the intercellular airspaces per unit leaf area ($S_c$), a measure for the surface area available for direct $CO_2$ exchange between the intercellular airspaces and the chloroplasts, and cell wall thickness ($T_{cw}$) (Fig. 3a,b). The mesophyll cell surface area facing the intercellular airspaces ($S_m$) also relates to $g_m$, but the relationship was generally weaker with $S_m$ than with $S_c$ (Fig. S5a). Across PFTs, larger values of $g_m$ are typically associated with a large $S_c$ and thinner cell walls (a small $T_{cw}$) and show a linear increase with $S_c$ and a nonlinear decrease with $T_{cw}$ (Fig. 3a,b). For a given $S_c$, herbaceous plants show a higher $g_m$ than other PFTs (Fig. 3a; Table S2). When looking at the mesophyll conductance per unit exposed chloroplast surface area ($g_{m,25}/S_c$) (Fig. 3c), it becomes apparent that the conductance per unit exposed chloroplast surface area decreases with increasing $T_{cw}$. Herbaceous PFTs have a larger $g_m$ per unit $S_c$ compared with woody plants or ferns. Although a significant relationship exists across PFTs, strong relationships within PFTs are generally missing, indicating that $T_{cw}$ does not explain a large amount of the variation in $g_m$ if differences in $S_c$ are accounted for. Most other leaf anatomical traits commonly reported in studies were not related to $g_m$: cytosol thickness ($T_{cytosol}$) and chloroplast thickness ($T_{chloroplast}$), as well as metrics describing chloroplast dimensions that did not show a statistically significant relationship with $g_m$ (Fig. S5), but in some cases also have a limited number of measurements.

Next, we addressed the question of how much of the variation in $g_m$ can be explained by these two most important anatomical traits. We applied a parsimonious generalised linear model to predict variations in $g_m$ in response to $T_{cw}$ and $S_c$ accounting for the gamma error distribution present in the $g_m$ data (please refer to e.g. Fig. 2a). The global model (all data pooled) indicates that these two anatomical traits can explain the variations in $g_m$ to a reasonable extent across PFTs ($R^2 = 0.48$; Table 1), which reflects the consistent global relationship evident in the pairwise plots of $g_m$ against $S_c$ and $T_{cw}$, respectively (Fig. 3a,b). For individual PFTs, model fits are good for all groups ($R^2 > 0.3$) except for annual herbaceous plants ($R^2 = 0.09$). In all cases, a greater $g_m$ was associated with a greater $S_c$ ($\beta_1 > 1$) and a smaller $T_{cw}$ ($\beta_2 < 1$). $S_c$ could be identified as a statistically significant variable ($P < 0.05$) in all PFTs except for annual herbaceous plants, whereas for $T_{cw}$ this was the case for all PFTs except deciduous angiosperms and annual herbs (Table 1).

What causes the large variation of $g_m$ in $C_3$ annual herbaceous plants? It is well established that $g_m$ is not only controlled by leaf anatomy, but also by biochemical factors such as aquaporin content and CA activity (Flexas *et al.*, 2018). However, since these

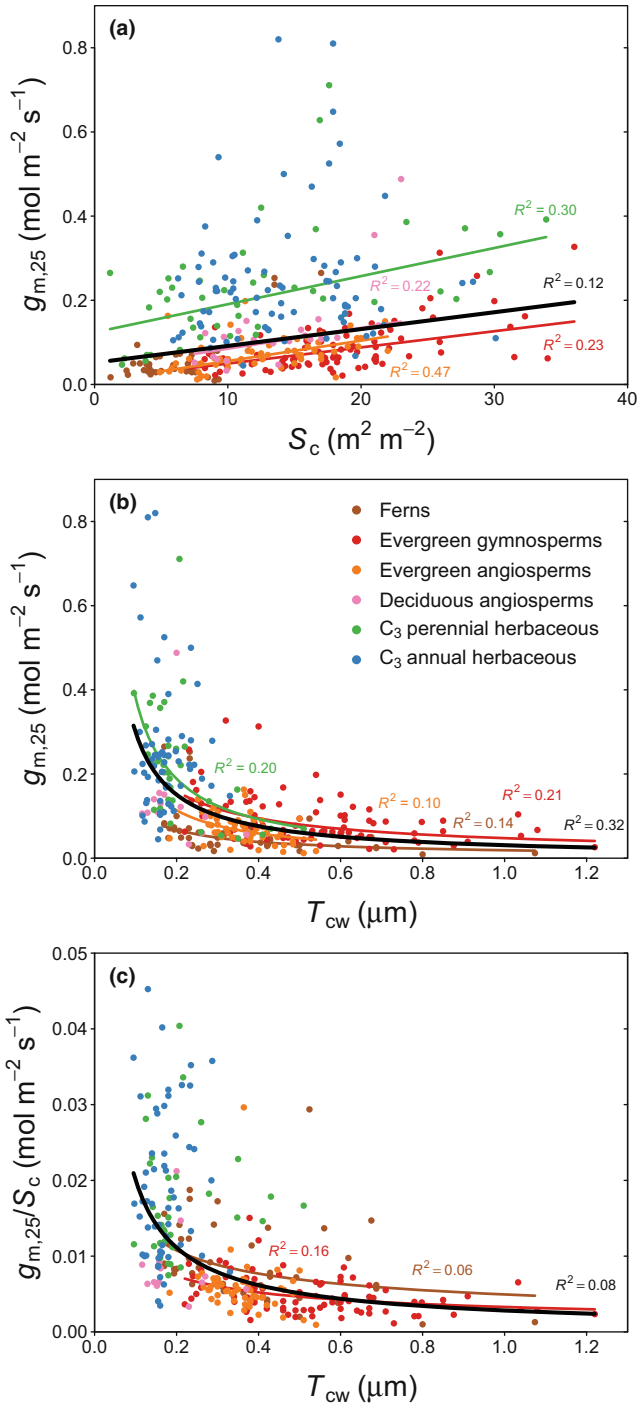


**Fig. 3** Mesophyll conductance standardised to 25°C ($g_{m,25}$) across plant functional types (PFTs) in relation to (a) chloroplast surface area exposed to the intercellular airspaces per unit leaf area ($S_c$), (b) cell wall thickness ($T_{cw}$), and (c) $g_{m,25}$ normalised by $S_c$ in relation to $T_{cw}$. Lines represent robust linear regression fits (panel a) and nonlinear regression fits of the form $y = ax^b$ (panels b, c), respectively, and were drawn if $P < 0.05$. Black lines represent global regression fits (all PFTs pooled).

factors are typically not measured or not reported in units that allow their intercomparison across studies, our analysis of biochemical leaf traits was limited to leaf nutrient as well as Rubisco contents. Nutrients integrate a wide range of functions within the leaf and therefore do not allow us to infer the immediate role of biochemical mechanisms on $g_m$. However, they are the only biochemical leaf traits that are frequently measured and reported in common units across studies.

Leaf nutrient concentrations for which enough common measurements with $g_m$ were available comprised leaf nitrogen (N) and potassium (K). Leaf N content per unit leaf area was well correlated with $g_{m,25}$ for $C_3$ annual herbaceous plants ($R^2$ = 0.51, $P < 0.001$) and showed moderate correlations with perennial herbaceous and deciduous angiosperm species, but not for evergreen woody plants (Fig. 4a). $C_3$ annual herbs and grasses also show a higher $g_{m,25}$ for the same amount of leaf N and a steeper slope, that is, a stronger increase in $g_{m,25}$ for a given increase in leaf N compared with other PFTs. Leaf K content per area was also positively related to $g_{m,25}$ in leaves of $C_3$ annual herbaceous plants across studies ($R^2$ = 0.44, $P < 0.01$). The limited availability of K content measurements did not allow us to investigate this relationship in other PFTs. While the number of concomitant $g_m$ and leaf K content measurements as depicted in Fig. 4(b) is relatively low ($n$ = 19), the relationship emerged across unstressed plants from 12 independent studies and is not merely the consequence of an individual experiment.

We next investigated whether the existing relationship between $g_{m,25}$ and leaf N was primarily caused by the N allocated to the enzyme Rubisco, which accounts for *c.* 20% of leaf N and constitutes the largest N pool in leaves (Evans & Clarke, 2019). A relationship between $g_{m,25}$ and Rubisco content would also indicate a coordination between $g_m$ and photosynthetic capacity ($V_{cmax}$), the two main variables which in combination determine the drawdown from $C_i$ to $C_c$. Therefore, we tested whether $g_m$ and $V_{cmax}$ are coordinated in a way to keep $C_c$, the available $CO_2$ concentration for carboxylation, or the ratio $C_c$ : $C_a$ relatively constant under unstressed conditions.

In contrast with $g_{m,25}$ and leaf N, we have found no statistically significant relationship ($P > 0.05$) between $g_{m,25}$ and leaf Rubisco content (Fig. 5a). The data also revealed that $V_{cmax,Cc}$, the 'true' carboxylation capacity of Rubisco derived from $A_n$–$C_c$ curves, is generally unrelated to $g_m$ across and within PFTs (Fig. 5b) with a large scatter in the reported $V_{cmax,Cc}$ for any given $g_m$. Herbaceous annual plants show a statistically significant positive relationship between $g_m$ and $V_{cmax,Cc}$ but only a weak correlation. The lack of coordination between $g_m$ and $V_{cmax,Cc}$ further results in a wide range of $C_i - C_c$ across species and a poorly constrained $C_c$ : $C_a$ ratio in unstressed leaves (Fig. 1d,f).

We further investigated whether and how the presented relationship between $g_m$ and $V_{cmax,Cc}$ differs across the three main measurement methods of $g_m$ (carbon isotopes, chlorophyll fluorescence and curve fitting). We found that $g_m$ measured with the carbon isotope technique showed a significantly higher correlation with $V_{cmax,Cc}$ compared with data measured with the fluorescence or curve fitting methods, in which a strong relationship between $g_m$ and $V_{cmax,Cc}$ is absent (Fig. 5c). The comparison further revealed that the ratio of $g_m$ to $V_{cmax,Cc}$ is greater when measured with the isotope method compared with the fluorescence method.

**Table 1** Model results of a generalised linear model (glm) of the form $\log(g_{m,25}) = \beta_0 + \beta_1 S_c + \beta_2 T_{cw}$, fitted with a gamma error distribution and a log-link function.

| | No. of studies | No. of measurements | Model coefficients | | | Model $R^2$ |
|---|---|---|---|---|---|---|
| | | | $\exp(\beta_0)$ | $\exp(\beta_1)$ | $\exp(\beta_2)$ | |
| All plant functional types | 50 | 295 | 0.128 (0.104, 0.158)*** | 1.050 (1.038, 1.063)*** | 0.096 (0.069, 0.133)*** | 0.48 |
| Ferns | 4 | 46 | 0.045 (0.025, 0.081)*** | 1.106 (1.056, 1.161)*** | 0.244 (0.097, 0.644)*** | 0.57 |
| Evergreen gymnosperms | 7 | 85 | 0.056 (0.037, 0.086)*** | 1.050 (1.033, 1.066)*** | 0.391 (0.253, 0.614)*** | 0.46 |
| Evergreen angiosperms | 10 | 57 | 0.091 (0.039, 0.216)*** | 1.046 (1.019, 1.075)** | 0.082 (0.012, 0.560)** | 0.34 |
| Deciduous angiosperms | 5 | 14 | 0.039 (0.010, 0.165)** | 1.093 (1.034, 1.159)* | 0.415 (0.005, 47.029) | 0.55 |
| $C_3$ perennial herbaceous | 10 | 34 | 0.254 (0.120, 0.548)** | 1.030 (1.004, 1.057)* | 0.051 (0.005, 0.590)* | 0.46 |
| $C_3$ annual herbaceous | 27 | 58 | 0.203 (0.087, 0.464)*** | 1.031 (0.997, 1.068). | 0.282 (0.012, 7.697) | 0.09 |

The model equation is equivalent to $g_{m,25} = \exp(\beta_0)\exp(\beta_1)^{Sc}\exp(\beta_2)^{Tcw}$, therefore the exponential function was applied to the model coefficients to allow their interpretation in the original scale of measurement. An increase of $S_c$ or $T_{cw}$ by one unit means that the expected value of $g_{m,25}$ is multiplied by $\exp(\beta_1)$ or $\exp(\beta_2)$, respectively. Values in brackets give the 95% confidence intervals of the coefficients. The $R^2$ represents McFadden's pseudo $R^2$ (please refer to the Materials and Methods section). Significance levels are denoted as follows: $P \leq 0.1$; *, $P \leq 0.05$; **, $P \leq 0.01$; ***, $P \leq 0.001$.

## Discussion

### Leaf structural and anatomical controls on mesophyll conductance

We conducted a literature analysis of mesophyll conductance ($g_m$) measurements with the aim of identifying traits that affect $g_m$ across and within PFTs. We found that leaf structural properties such as LMA, leaf thickness, leaf density and leaf porosity were poorly associated with $g_m$ for any PFT. This lack of association most probably reflects the integrative nature of these traits. For example, LMA is a product of leaf thickness and density, both of which can vary due to modifications in different underlying traits such as $T_{cw}$ or $S_m$ (Poorter *et al.*, 2009; Onoda *et al.*, 2017) with potentially opposing effects on $g_m$ (Onoda *et al.*, 2017). By contrast, anatomical traits such as $S_c$ and $T_{cw}$ are expected to have a much more direct effect on $g_m$ and have previously been identified as important anatomical determinants for leaf internal $CO_2$ transfer in all plant groups (Tosens *et al.*, 2016; Ouyang *et al.*, 2017; Xiong *et al.*, 2017; Veromann-Jürgenson *et al.*, 2020). In this analysis, $T_{cw}$ and $S_c$ explained approximately half of the variation in $g_m$ globally (i.e. all data pooled) as well as within most PFTs, including ferns, evergreen gymnosperms and perennial herbs. Nonetheless, other leaf anatomical traits for which we did not have sufficient data might also play an important role for $g_m$. Differences in cell wall composition and associated changes in effective cell wall porosity (porosity/tortuosity) have been shown to affect $g_m$ (Ellsworth *et al.*, 2018; Carriquí *et al.*, 2020; Flexas *et al.*, 2021), and may explain the observed variations in $g_m/S_c$ for a given $T_{cw}$ (Evans, 2021). Notably, our results indicate a much smaller role of leaf anatomical traits in herbaceous annuals compared with other

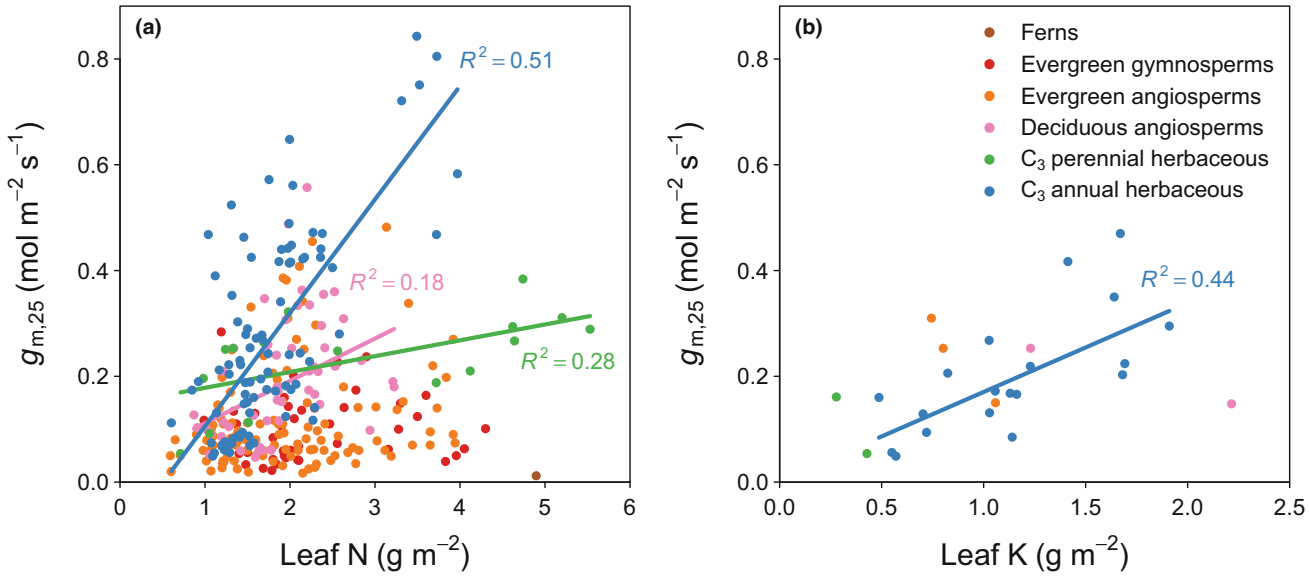


**Fig. 4** Relationship between mesophyll conductance standardised to 25°C ($g_{m,25}$) and (a) leaf nitrogen (N) content, and (b) leaf potassium (K) content. Lines represent robust linear regression fits and were drawn if $P < 0.05$.

PFTs, which suggests a higher relative importance of traits other than leaf anatomy in this group.

The distinction between leaf structural and leaf anatomical traits also allows some insights into the relative importance of gas and liquid-phase diffusion components of $g_m$. Leaf structural traits such as leaf and mesophyll thickness, leaf density, and in particular leaf porosity are expected to be related to $CO_2$ transfer conductance in the gaseous phase, whereas anatomical traits such as $T_{cw}$ and $S_c$, but also biochemical factors play a role mainly for $CO_2$ transfer in the liquid phase (Niinemets & Reichstein, 2003; Nobel, 2020). The fact that none of the structural leaf traits were related to $g_m$ within or across PFTs indicates that $CO_2$ diffusion in the gas phase is of minor importance compared with $CO_2$ transfer in the liquid phase. This view is supported by modelling studies, which assign the largest fraction of the total resistance to the liquid phase throughout PFTs (Tomás *et al.*, 2013; Peguero-Pina *et al.*, 2016; Du *et al.*, 2019; Carriquí *et al.*, 2020).

## Leaf biochemical controls on mesophyll conductance

We found that $g_m$ is strongly correlated with leaf N and K contents in herbaceous annual plants, moderately correlated with leaf N content in herbaceous perennials and deciduous angiosperms, but uncorrelated with leaf N content in woody evergreens. These findings mirror the current state of the literature. While there is generally a positive association between nutrients and $g_m$ in woody evergreens, this is in many cases not significant (Warren, 2004; Bown *et al.*, 2009; Battie-Laclau *et al.*, 2014). However, experimental studies focusing on nutrient effects in woody evergreens are also less common than those studying herbaceous species. For herbaceous annuals there is strong evidence that leaf macro-nutrients have positive effects on $g_m$. This is not only apparent for unstressed leaves across studies (Fig. 4), but it is also a common observation within studies that have considered nutrients as treatment factors. Studies that supplied plants with varying amounts of N usually find a positive association between leaf N content and $g_m$ in herbaceous plant species (Yamori *et al.*, 2011; Li *et al.*, 2013; Hu *et al.*, 2019; Cai *et al.*, 2020). Similarly, higher leaf K content is associated with higher $g_m$ in a wide range of studies (Lu *et al.*, 2016, 2019; Hou *et al.*, 2018; Hu *et al.*, 2019; Xie *et al.*, 2020).

The question remains what underlying biochemical mechanisms cause the clear positive relationship between $g_m$ and leaf N and K content in herbaceous annuals? As leaf N and K control a

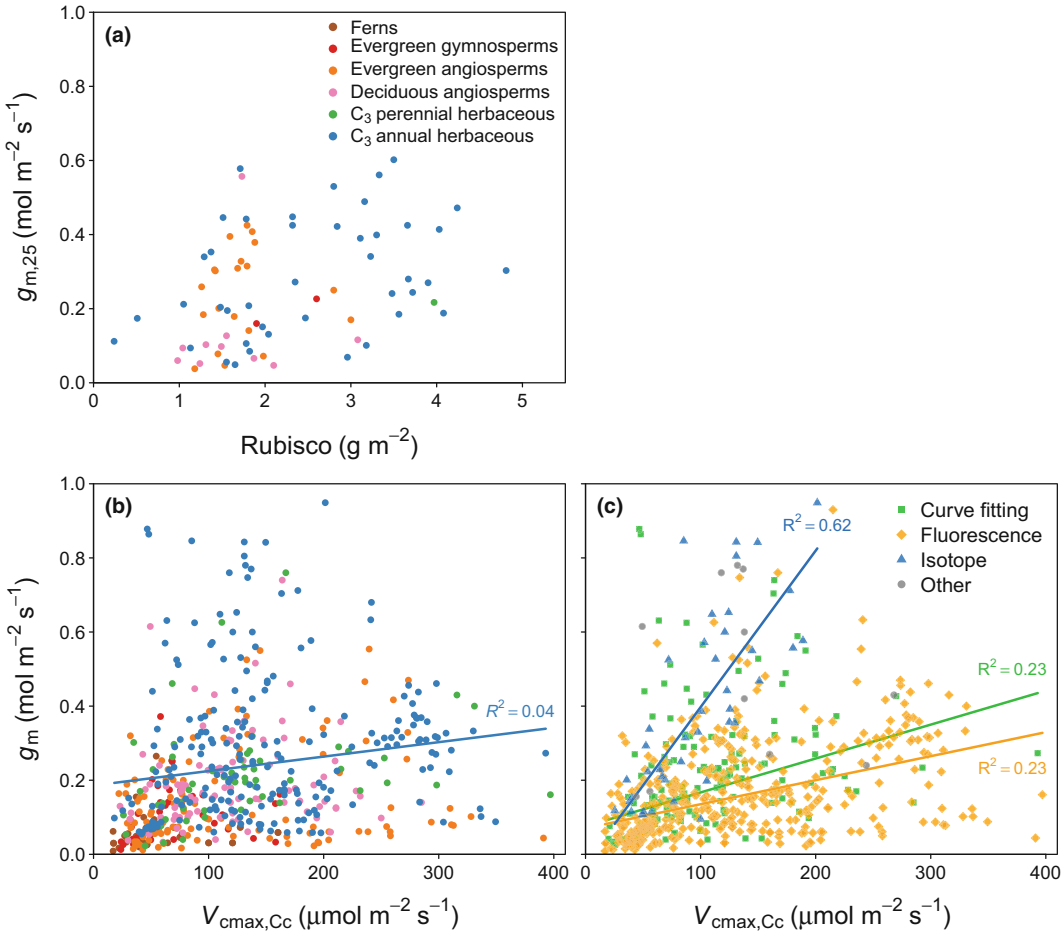


**Fig. 5** Relationship between mesophyll conductance standardised to 25°C ($g_{m,25}$) and (a) leaf Rubisco content, (b) maximum carboxylation rate derived from $A_n$–$C_c$ curves ($V_{cmax,Cc}$) and (c) same as (b) but data grouped by the measurement method applied. $g_m$ and $V_{cmax,Cc}$ in panels (b, c) were measured at the same temperature. Lines represent robust linear regression fits and were drawn if $P < 0.05$.

vast spectrum of biochemical functions inside the leaf (Wang *et al.*, 2016; Evans & Clarke, 2019) we could not attribute leaf N and K content to individual biochemical mechanisms that directly affect $g_m$. Biochemical factors that have long been suggested as possible determinants for $g_m$ are aquaporins and CA (Hanba *et al.*, 2004; Warren, 2008), proteins that regulate $CO_2$ transfer through cell membranes and through the cytosol and the chloroplast stroma, respectively. A positive effect on $g_m$ has been demonstrated for aquaporins (Hanba *et al.*, 2004; Flexas *et al.*, 2006; Perez-Martin *et al.*, 2014; Xu *et al.*, 2019; but see Kromdijk *et al.*, 2020) and to a lesser extent for CA activity (Perez-Martin *et al.*, 2014; Momayyezi & Guy, 2017). There is further limited evidence that leaf N and K are positively associated with the expression of aquaporins (Armengaud *et al.*, 2004; Wang *et al.*, 2016; Ding *et al.*, 2018; Zhu *et al.*, 2020) as well as CA activity (Makino *et al.*, 1992; Mohammad & Naseem, 2006; Siddiqui *et al.*, 2008). However, contrasting results have been reported (Ding *et al.*, 2016) and clearly a better understanding of nutrient effects on leaf biochemical functioning is needed (Gao *et al.*, 2018). Effects of leaf N on $g_m$ may also be indirect through changes in leaf anatomical traits as well as photosynthetic capacity with leaf N content. However, the fact that neither leaf anatomy nor Rubisco content could explain a large proportion of the variance in $g_m$ in herbaceous annual plants points to leaf biochemical factors associated with membranes and cytosol as well as stromal components as more important regulators of $g_m$ in this group.

### Relative importance of anatomical and biochemical factors across PFTs

Our findings provide strong indications that biochemical and anatomical factors are of contrasting importance for $g_m$ across PFTs. We found that anatomical factors explain a substantial fraction of the variation in $g_m$ in all PFTs except annual herbaceous plants. In the latter group, only leaf nutrients could be related to $g_m$, which in turn were less relevant in other PFTs. Therefore, our results suggest that in annual herbaceous plants leaf biochemical mechanisms associated with leaf nutrients are relatively more important in explaining $g_m$ across species compared with leaf anatomical traits. Although these results do not imply that biochemical factors constitute a relevant mechanism solely in annual herbs, they suggest that their relative importance for explaining $g_m$ is higher in this plant group compared with other PFTs. A more prominent role of nonanatomical components for $g_m$ in annual herbs compared with leaf anatomical features is also suggested by leaf-level modelling analyses (Tomás *et al.*, 2013; Tosens & Laanisto, 2018), and it would be relevant to investigate in how far phylogenetic effects contribute to these differences. Studies looking at changes in $g_m$ over the course of an experimental treatment (e.g. drought or nutrient stress) have further provided evidence of PFT-dependent variations in the share of anatomical and biochemical controls on $g_m$. While in some cases changes in $g_m$ were linked to leaf anatomical traits (Lu *et al.*, 2016; Xie *et al.*, 2020), other studies have argued that variations in $g_m$ could be better explained by changes in leaf biochemistry (Hanba *et al.*, 2004; Miyazawa *et al.*, 2008; Xiong & Flexas, 2021), which is more in line with the findings in this study.

### Implications for enhancing photosynthesis

We analysed published data on photosynthetic limitation as defined by Farquhar & Sharkey (1982), an approach that quantifies the photosynthetic limitation caused by $g_m$ ($L_m$) given the coexisting limitations imposed by stomata and leaf photosynthetic capacity. Our results emphasise the possible underestimated potential of $g_m$ for improving photosynthesis by increasing the available $CO_2$ concentration at the sites of carboxylation ($C_c$). This does not only apply to PFTs with inherently low $CO_2$ diffusion conductance, but also to herbaceous annual crops, which show the highest $g_m$ values of all plant types. Representative $g_m$ values measured in crop species under unstressed conditions (*c.* 0.26 mol $m^{-2}$ $s^{-1}$) imply a limitation to photosynthesis that can be attributed to $g_m$ of *c.* 20% under ambient $CO_2$ concentrations, but this percentage is likely to be higher in some crop species such as rice, bean, tomato or soybean, which show a relatively low $g_m$ compared with other crops (Fig. S3). The values compiled here further suggest that an increase of $g_m$ in crops from 0.26 to 0.42 mol $m^{-2}$ $s^{-1}$ (i.e. from the median to the 75$^{th}$ percentile) has the potential to increase photosynthesis by *c.* 8%, with probable positive effects on crop productivity and yields (Xu *et al.*, 2019).

How could an increase in $g_m$ be achieved in annual crops? Based on our results we argue that plant engineering and breeding efforts targeting biochemical leaf properties (Groszmann *et al.*, 2017; Lundgren & Fleming, 2020) are more promising than those that focus on anatomical traits (e.g. engineering for thinner cell walls) (Tholen *et al.*, 2012), which would probably have limited effects on $g_m$ in crops. The most promising factors in that respect are those that facilitate $CO_2$ transfer across membranes, cytosol and stromal components such as CA activity and aquaporins. The fact that good correlations between $g_m$ and light-saturated photosynthesis have been observed throughout the literature (e.g. Evans *et al.*, 1994; Centritto *et al.*, 2009; Fullana-Pericàs *et al.*, 2017) also suggests that increases in Rubisco content and/or Rubisco properties such as $V_{cmax}$ are able to increase $g_m$. However, we found that the true carboxylation capacity of Rubisco, that is the $C_c$-based $V_{cmax}$ ($V_{cmax,Cc}$), does not or only poorly correlate with $g_m$ across and within PFTs, which corroborates findings from earlier data compilations (Ethier & Livingston, 2004; Warren & Adams, 2006). Consequently, an increase in $V_{cmax,Cc}$ (and therefore a higher rate of $CO_2$ consumption) is not necessarily concomitant with an enhanced supply rate of $CO_2$ through increased $g_m$, an observation that was supported by a widely varying $C_i - C_c$ and $C_c/C_a$ in unstressed plants. These results imply that plant engineering efforts that focus solely on enhancing Rubisco catalytic rate (Galmés *et al.*, 2019), one of the suggested main pathways for improving photosynthesis (Long *et al.*, 2006), are likely to be less effective in increasing photosynthetic productivity than parallel increases in both $g_m$ and Rubisco activity, which would enhance both $CO_2$ demand and supply.

### Pathways for future research

The dataset presented here gives unprecedented insights into the extent of photosynthetic limitation imposed by $g_m$ as well as its anatomical and biochemical controlling factors across PFTs. The results from this meta-analysis further have the potential to motivate future research activities. Our findings strongly suggest that the sources of disagreement among measurement methods of $g_m$ deserve further scrutiny. In particular the causes of the differences between the two widely established isotope and fluorescence methods and their relationship with $V_{cmax,Cc}$ need to be resolved to not critically confound findings as reported here and in other meta-analyses (e.g. Onoda *et al.*, 2017; Gago *et al.*, 2019; Ren *et al.*, 2019), which usually pool $g_m$ measurements across methods. Similarly, the effects of other sources of variation in the data, such as species, growth conditions or growth stages need to be investigated in more detail.

We further argue that a better mechanistic understanding of the factors underpinning the results reported here are urgently required. Particularly the potential links between leaf nutrients and biochemical mechanisms affecting $CO_2$ diffusion inside leaves need to be better understood. We suggest that controlled experiments in combination with the latest leaf-level modelling approaches (Tholen & Zhu, 2011; Xiao & Zhu, 2017) will be best suited to elucidate the role of individual biochemical and anatomical leaf traits for $g_m$ across PFTs.

## Acknowledgements

The Estonian Research Council has supported the work of TT and L-LV-J (PUT 1473) and ÜN (PRG 537). MC was supported by a grant overseen by the French National Research Agency (ANR) as part of the 'Investissements d'Avenir' program (ANR-11-LABX-0002-01, Laboratory of Excellence ARBRE). MC and CW were also supported by a grant from the German Research Foundation (DFG, CU 173/4-1, WE 2681/10-1). We are grateful to Jeff Powell for useful discussions.

## Author contributions

JK designed the study, compiled and analysed the data and wrote the manuscript. JRE contributed to data analysis. L-LV-J, TT and ÜN contributed data. All coauthors (MC, ÜN, TT, L-LV-J, CW, SZ) contributed to the interpretation of the data, the presentation of the results, and the writing of the manuscript.

## ORCID

Matthias Cuntz https://orcid.org/0000-0002-5966-1829
John R. Evans https://orcid.org/0000-0003-1379-3532
Jürgen Knauer https://orcid.org/0000-0002-4947-7067
Ülo Niinemets https://orcid.org/0000-0002-3078-2192
Tiina Tosens https://orcid.org/0000-0003-3802-2478
Linda-Liisa Veromann-Jürgenson https://orcid.org/0000-0001-7801-5083
Christiane Werner https://orcid.org/0000-0002-7676-9057
Sönke Zaehle https://orcid.org/0000-0001-5602-7956

## Data availability

All data presented in this manuscript are publicly available via Figshare (Knauer *et al.*, 2022).

## References

**Armengaud P, Breitling R, Amtmann A. 2004.** The potassium-dependent transcriptome of Arabidopsis reveals a prominent role of jasmonic acid in nutrient signaling. *Plant Physiology* **136**: 2556–2576.

**Battie-Laclau P, Laclau J-P, Beri C, Mietton L, Muniz MRA, Arenque BC, de Cassia PM, Jordan-Meille L, Bouillet J-P, Nouvellon Y. 2014.** Photosynthetic and anatomical responses of *Eucalyptus grandis* leaves to potassium and sodium supply in a field experiment. *Plant, Cell & Environment* **37**: 70–81.

**Berghuijs HN, Yin X, Ho QT, van der Putten PE, Verboven P, Retta MA, Nicolaï BM, Struik PC. 2015.** Modelling the relationship between $CO_2$ assimilation and leaf anatomical properties in tomato leaves. *Plant Science* **238**: 297–311.

**Bernacchi CJ, Portis AR, Nakano H, von Caemmerer S, Long SP. 2002.** Temperature response of mesophyll conductance. Implications for the determination of Rubisco enzyme kinetics and for limitations to photosynthesis *in vivo*. *Plant Physiology* **130**: 1992–1998.

**Bown HE, Watt MS, Mason EG, Clinton PW, Whitehead D. 2009.** The influence of nitrogen and phosphorus supply and genotype on mesophyll conductance limitations to photosynthesis in *Pinus radiata*. *Tree Physiology* **29**: 1143–1151.

**von Caemmerer S, Evans JR. 2010.** Enhancing $C_3$ photosynthesis. *Plant Physiology* **154**: 589–592.

**Cai C, Li G, Di L, Ding Y, Fu L, Guo X, Struik PC, Pan G, Li H, Chen W *et al.* 2020.** The acclimation of leaf photosynthesis of wheat and rice to seasonal temperature changes in T-FACE environments. *Global Change Biology* **26**: 539–556.

**Carriquí M, Nadal M, Clemente-Moreno MJ, Gago J, Miedes E, Flexas J. 2020.** Cell wall composition strongly influences mesophyll conductance in gymnosperms. *The Plant Journal* **103**: 1372–1385.

**Centritto M, Lauteri M, Monteverdi MC, Serraj R. 2009.** Leaf gas exchange, carbon isotope discrimination, and grain yield in contrasting rice genotypes subjected to water deficits during the reproductive stage. *Journal of Experimental Botany* **60**: 2325–2339.

**Ding L, Gao L, Liu W, Wang M, Gu M, Ren B, Xu G, Shen Q, Guo S. 2016.** Aquaporin plays an important role in mediating chloroplastic $CO_2$ concentration under high-N supply in rice (*Oryza sativa*) plants. *Physiologia Plantarum* **156**: 215–226.

**Ding L, Li Y, Gao L, Lu Z, Wang M, Ling N, Shen Q, Guo S. 2018.** Aquaporin expression and water transport pathways inside leaves are affected by nitrogen supply through transpiration in rice plants. *International Journal of Molecular Sciences* **19**: 256.

**Du Q, Liu T, Jiao X, Song X, Zhang J, Li J. 2019.** Leaf anatomical adaptations have central roles in photosynthetic acclimation to humidity. *Journal of Experimental Botany* **70**: 4949–4962.

**Elferjani R, Benomar L, Momayyezi M, Tognetti R, Niinemets Ü, Soolanayakanahally RY, Théroux-Rancourt G, Tosens T, Ripullone F, Bilodeau-Gauthier S *et al.* 2021.** A meta-analysis of mesophyll conductance to $CO_2$ in relation to major abiotic stresses in poplar species. *Journal of Experimental Botany* **72**: 4384–4400.

**Ellsworth PV, Ellsworth PZ, Koteyeva NK, Cousins AB. 2018.** Cell wall properties in *Oryza sativa* influence mesophyll $CO_2$ conductance. *New Phytologist* **219**: 66–76.

**Epron D, Godard D, Cornic G, Genty B. 1995.** Limitation of net $CO_2$ assimilation rate by internal resistances to $CO_2$ transfer in the leaves of two tree species (*Fagus sylvatica* L. and *Castanea sativa* Mill.). *Plant, Cell & Environment* **18**: 43–51.

**Ethier GJ, Livingston NJ. 2004.** On the need to incorporate sensitivity to $CO_2$ transfer conductance into the Farquhar-von Caemmerer-Berry leaf photosynthesis model. *Plant, Cell & Environment* **27**: 137–153.

**Evans JR. 2021.** Mesophyll conductance: walls, membranes and spatial complexity. *New Phytologist* **229**: 1864–1876.

**Evans JR, Caemmerer S, Setchell BA, Hudson GS. 1994.** The relationship between $CO_2$ transfer conductance and leaf anatomy in transgenic tobacco with a reduced content of Rubisco. *Functional Plant Biology* **21**: 475–495.

**Evans JR, Clarke VC. 2019.** The nitrogen cost of photosynthesis. *Journal of Experimental Botany* **70**: 7–15.

**Evans JR, Kaldenhoff R, Genty B, Terashima I. 2009.** Resistances along the $CO_2$ diffusion pathway inside leaves. *Journal of Experimental Botany* **60**: 2235–2248.

**Evans JR, von Caemmerer S. 2013.** Temperature response of carbon isotope discrimination and mesophyll conductance in tobacco. *Plant, Cell & Environment* **36**: 745–756.

**Fabre N, Reiter IM, Becuwe-Linka N, Genty B, Rumeau D. 2007.** Characterization and expression analysis of genes encoding α and β carbonic anhydrases in Arabidopsis. *Plant, Cell & Environment* **30**: 617–629.

**Farquhar GD, Sharkey TD. 1982.** Stomatal conductance and photosynthesis. *Annual Review of Plant Physiology* **33**: 317–345.

**Flexas J, Barbour MM, Brendel O, Cabrera HM, Carriquí M, Díaz-Espejo A, Douthe C, Dreyer E, Ferrio JP, Gago J *et al.* 2012.** Mesophyll diffusion conductance to $CO_2$: an unappreciated central player in photosynthesis. *Plant Science* **193**: 70–84.

**Flexas J, Cano FJ, Carriquí M, Coopman RE, Mizokami Y, Tholen D, Xiong D. 2018.** $CO_2$ diffusion inside photosynthetic organs. In: Adams WW III, Terashima I, eds. *Advances in photosynthesis and respiration. The leaf: a platform for performing photosynthesis*. Cham, Switzerland: Springer International, 163–208.

**Flexas J, Clemente-Moreno MJ, Bota J, Brodribb TJ, Gago J, Mizokami Y, Nadal M, Perera-Castro AV, Roig-Oliver M, Sugiura D *et al.* 2021.** Cell wall thickness and composition are involved in photosynthetic limitation. *Journal of Experimental Botany* **72**: 3971–3986.

**Flexas J, Ribas-Carbó M, Hanson DT, Bota J, Otto B, Cifre J, McDowell N, Medrano H, Kaldenhoff R. 2006.** Tobacco aquaporin NtAQP1 is involved in mesophyll conductance to $CO_2$ *in vivo*. *The Plant Journal* **48**: 427–439.

**Fullana-Pericàs M, Conesa M, Soler S, Ribas-Carbó M, Granell A, Galmés J. 2017.** Variations of leaf morphology, photosynthetic traits and water-use efficiency in Western-Mediterranean tomato landraces. *Photosynthetica* **55**: 121–133.

**Gago J, Carriquí M, Nadal M, Clemente-Moreno MJ, Coopman RE, Fernie AR, Flexas J. 2019.** Photosynthesis optimized across land plant phylogeny. *Trends in Plant Science* **24**: 947–958.

**Gago J, Daloso DM, Carriquí M, Nadal M, Morales M, Araújo WL, Nunes-Nesi A, Flexas J. 2020.** Mesophyll conductance: the leaf corridors for photosynthesis. *Biochemical Society Transactions* **48**: 429–439.

**Galmés J, Capó-Bauçà S, Niinemets Ü, Iñiguez C. 2019.** Potential improvement of photosynthetic $CO_2$ assimilation in crops by exploiting the natural variation in the temperature response of Rubisco catalytic traits. *Current Opinion in Plant Biology* **49**: 60–67.

**Gao L, Lu Z, Ding L, Guo J, Wang M, Ling N, Guo S, Shen Q. 2018.** Role of aquaporins in determining carbon and nitrogen status in higher plants. *International Journal of Molecular Sciences* **19**: 35.

**Grassi G, Magnani F. 2005.** Stomatal, mesophyll conductance and biochemical limitations to photosynthesis as affected by drought and leaf ontogeny in ash and oak trees. *Plant, Cell & Environment* **28**: 834–849.

**Groszmann M, Osborn HL, Evans JR. 2017.** Carbon dioxide and water transport through plant aquaporins. *Plant, Cell & Environment* **40**: 938–961.

**Hanba YT, Shibasaka M, Hayashi Y, Hayakawa T, Kasamo K, Terashima I, Katsuhara M. 2004.** Overexpression of the barley aquaporin HvPIP2;1 increases internal $CO_2$ conductance and $CO_2$ assimilation in the leaves of transgenic rice plants. *Plant and Cell Physiology* **45**: 521–529.

**Hou W, Yan J, Jákli B, Lu J, Ren T, Cong R, Li X. 2018.** Synergistic effects of nitrogen and potassium on quantitative limitations to photosynthesis in rice (*Oryza sativa* L.). *Journal of Agricultural and Food Chemistry* **66**: 5125–5132.

**Hu W, Ren T, Meng F, Cong R, Li X, White PJ, Lu J. 2019.** Leaf photosynthetic capacity is regulated by the interaction of nitrogen and potassium through coordination of $CO_2$ diffusion and carboxylation. *Physiologia Plantarum* **167**: 418–432.

**Knauer J, Cuntz M, Evans JR, Niinemets Ü, Tosens T, Veromann-Jürgenson L-L, Werner C, Zaehle S. 2022.** A global dataset of mesophyll conductance measurements and accompanying leaf traits. *Figshare*. doi: 10.6084/m9.figshare.19681410.v1

**Knauer J, Zaehle S, De Kauwe MG, Bahar NHA, Evans JR, Medlyn BE, Reichstein M, Werner C. 2019.** Effects of mesophyll conductance on vegetation responses to elevated $CO_2$ concentrations in a land surface model. *Global Change Biology* **25**: 1820–1838.

**Knauer J, Zaehle S, De Kauwe MG, Haverd V, Reichstein M, Sun Y. 2020.** Mesophyll conductance in land surface models: effects on photosynthesis and transpiration. *The Plant Journal* **101**: 858–873.

**Kromdijk J, Głowacka K, Long SP. 2020.** Photosynthetic efficiency and mesophyll conductance are unaffected in *Arabidopsis thaliana* aquaporin knock-out lines. *Journal of Experimental Botany* **71**: 318–329.

**Li Y, Ren B, Ding L, Shen Q, Peng S, Guo S. 2013.** Does chloroplast size influence photosynthetic nitrogen use efficiency? *PLoS ONE* **8**: e62036.

**Long SP, Zhu X-G, Naidu SL, Ort DR. 2006.** Can improvement in photosynthesis increase crop yields? *Plant, Cell & Environment* **29**: 315–330.

**Lu Z, Lu J, Pan Y, Lu P, Li X, Cong R, Ren T. 2016.** Anatomical variation of mesophyll conductance under potassium deficiency has a vital role in determining leaf photosynthesis. *Plant, Cell & Environment* **39**: 2428–2439.

**Lu Z, Xie K, Pan Y, Ren T, Lu J, Wang M, Shen Q, Guo S. 2019.** Potassium mediates coordination of leaf photosynthesis and hydraulic conductance by modifications of leaf anatomy. *Plant, Cell & Environment* **42**: 2231–2244.

**Lundgren MR, Fleming AJ. 2020.** Cellular perspectives for improving mesophyll conductance. *The Plant Journal* **101**: 845–857.

**Maechler M, Rousseeuw P, Croux C, Todorov V, Ruckstuhl A, Salibian-Barrera M, Verbeke T, Koller M, Conceicao ELT, Di Palma MA. 2022.** *Robustbase: basic robust statistics*. R package v.0.95-0. [WWW document] URL http://CRAN.R-project.org/package=robustbase [accessed 3 June 2022].

**Makino A, Sakashita H, Hidema J, Mae T, Ojima K, Osmond B. 1992.** Distinctive responses of ribulose-1, 5-bisphosphate carboxylase and carbonic anhydrase in wheat leaves to nitrogen nutrition and their possible relationships to $CO_2$-transfer resistance. *Plant Physiology* **100**: 1737–1743.

**Miyazawa S-I, Yoshimura S, Shinzaki Y, Maeshima M, Miyake C. 2008.** Deactivation of aquaporins decreases internal conductance to $CO_2$ diffusion in tobacco leaves grown under long-term drought. *Functional Plant Biology* **35**: 553–564.

**Mohammad F, Naseem U. 2006.** Effect of K application on leaf carbonic anhydrase and nitrate reductase activities, photosynthetic characteristics, NPK and $NO_3$ contents, growth, and yield of mustard. *Photosynthetica* **44**: 471–473.

**Momayyezi M, Guy RD. 2017.** Substantial role for carbonic anhydrase in latitudinal variation in mesophyll conductance of *Populus trichocarpa* Torr. & Gray. *Plant, Cell & Environment* **40**: 138–149.

**Niinemets Ü, Díaz-Espejo A, Flexas J, Galmés J, Warren CR. 2009.** Importance of mesophyll diffusion conductance in estimation of plant photosynthesis in the field. *Journal of Experimental Botany* **60**: 2271–2282.

**Niinemets Ü, Reichstein M. 2003.** Controls on the emission of plant volatiles through stomata: a sensitivity analysis. *Journal of Geophysical Research: Atmospheres* **108**: 4211.

**Nobel PS. 2020.** *Physicochemical & environmental plant physiology*. London, UK: Elsevier Academic Press.

**Ogle DH, Doll JC, Wheeler P, Dinno A. 2022.** *FSA: fisheries stock analysis*. R package v.0.9.3. [WWW document] URL https://github.com/fishR-Core-Team/FSA [accessed 3 June 2022].

**Onoda Y, Wright IJ, Evans JR, Hikosaka K, Kitajima K, Niinemets Ü, Poorter H, Tosens T, Westoby M. 2017.** Physiological and structural tradeoffs underlying the leaf economics spectrum. *New Phytologist* **214**: 1447–1463.

**Ort DR, Merchant SS, Alric J, Barkan A, Blankenship RE, Bock R, Croce R, Hanson MR, Hibberd JM, Long SP *et al.* 2015.** Redesigning photosynthesis to sustainably meet global food and bioenergy demand. *Proceedings of the National Academy of Sciences, USA* **112**: 8529–8536.

**Ouyang W, Struik PC, Yin X, Yang J. 2017.** Stomatal conductance, mesophyll conductance, and transpiration efficiency in relation to leaf anatomy in rice and wheat genotypes under drought. *Journal of Experimental Botany* **68**: 5191–5205.

**Peguero-Pina JJ, Sisó S, Sancho-Knapik D, Díaz-Espejo A, Flexas J, Galmés J, Gil-Pelegrín E. 2016.** Leaf morphological and physiological adaptations of a

deciduous oak (*Quercus faginea* Lam.) to the Mediterranean climate: a comparison with a closely related temperate species (*Quercus robur* L.). *Tree Physiology* **36**: 287–299.

**Perez-Martin A, Michelazzo C, Torres-Ruiz JM, Flexas J, Fernández JE, Sebastiani L, Diaz-Espejo A. 2014.** Regulation of photosynthesis and stomatal and mesophyll conductance under water stress and recovery in olive trees: correlation with gene expression of carbonic anhydrase and aquaporins. *Journal of Experimental Botany* **65**: 3143–3156.

**Pons TL, Flexas J, Von Caemmerer S, Evans JR, Genty B, Ribas-Carbo M, Brugnoli E. 2009.** Estimating mesophyll conductance to $CO_2$: methodology, potential errors, and recommendations. *Journal of Experimental Botany* **60**: 2217–2234.

**Poorter H, Niinemets Ü, Poorter L, Wright IJ, Villar R. 2009.** Causes and consequences of variation in leaf mass per area (LMA): a meta-analysis. *New Phytologist* **182**: 565–588.

**R Core Team. 2021.** *R: a language and environment for statistical computing*. Vienna, Austria: R Foundation for Statistical Computing.

**Ren T, Weraduwage SM, Sharkey TD. 2019.** Prospects for enhancing leaf photosynthetic capacity by manipulating mesophyll cell morphology. *Journal of Experimental Botany* **70**: 1153–1165.

**Siddiqui MH, Khan MN, Mohammad F, Khan MMA. 2008.** Role of nitrogen and gibberellin ($GA_3$) in the regulation of enzyme activities and in osmoprotectant accumulation in *Brassica juncea* L. under salt stress. *Journal of Agronomy and Crop Science* **194**: 214–224.

**Sun Y, Gu L, Dickinson RE, Norby RJ, Pallardy SG, Hoffman FM. 2014.** Impact of mesophyll diffusion on estimated global land $CO_2$ fertilization. *Proceedings of the National Academy of Sciences, USA* **111**: 15774–15779.

**Tholen D, Boom C, Zhu X-G. 2012.** Opinion: prospects for improving photosynthesis by altering leaf anatomy. *Plant Science* **197**: 92–101.

**Tholen D, Zhu X-G. 2011.** The mechanistic basis of internal conductance: a theoretical analysis of mesophyll cell photosynthesis and $CO_2$ diffusion. *Plant Physiology* **156**: 90–105.

**Tomás M, Flexas J, Copolovici L, Galmés J, Hallik L, Medrano H, Ribas-Carbó M, Tosens T, Vislap V, Niinemets Ü. 2013.** Importance of leaf anatomy in determining mesophyll diffusion conductance to $CO_2$ across species: quantitative limitations and scaling up by models. *Journal of Experimental Botany* **64**: 2269–2281.

**Tosens T, Nishida K, Gago J, Coopman RE, Cabrera HM, Carriquí M, Laanisto L, Morales L, Nadal M, Rojas R *et al.* 2016.** The photosynthetic capacity in 35 ferns and fern allies: mesophyll $CO_2$ diffusion as a key trait. *New Phytologist* **209**: 1576–1590.

**Tosens T, Laanisto L. 2018.** Mesophyll conductance and accurate photosynthetic carbon gain calculations. *Journal of Experimental Botany* **69**: 5315–5318.

**Uehlein N, Lovisolo C, Siefritz F, Kaldenhoff R. 2003.** The tobacco aquaporin NtAQP1 is a membrane $CO_2$ pore with physiological functions. *Nature* **425**: 734–737.

**Veromann-Jürgenson L-L, Brodribb TJ, Niinemets Ü, Tosens T. 2020.** Variability in chloroplast area lining intercellular airspace and cell walls drive mesophyll conductance in gymnosperms. *Journal of Experimental Botany* **71**: 4958–4971.

**Walker B, Ariza LS, Kaines S, Badger MR, Cousins AB. 2013.** Temperature response of in vivo Rubisco kinetics and mesophyll conductance in *Arabidopsis thaliana*: comparisons to *Nicotiana tabacum*. *Plant, Cell & Environment* **36**: 2108–2119.

**Wang M, Ding L, Gao L, Li Y, Shen Q, Guo S. 2016.** The interactions of aquaporins and mineral nutrients in higher plants. *International Journal of Molecular Sciences* **17**: 1229.

**Warren C, Ethier G, Livingston N, Grant N, Turpin D, Harrison D, Black T. 2003.** Transfer conductance in second growth Douglas-fir (*Pseudotsuga menziesii* (Mirb.) Franco) canopies. *Plant, Cell & Environment* **26**: 1215–1227.

**Warren CR. 2004.** The photosynthetic limitation posed by internal conductance to $CO_2$ movement is increased by nutrient supply. *Journal of Experimental Botany* **55**: 2313–2321.

**Warren CR. 2008.** Stand aside stomata, another actor deserves centre stage: the forgotten role of the internal conductance to $CO_2$ transfer. *Journal of Experimental Botany* **59**: 1475–1487.

**Warren CR, Adams MA. 2006.** Internal conductance does not scale with photosynthetic capacity: implications for carbon isotope discrimination and the economics of water and nitrogen use in photosynthesis. *Plant, Cell & Environment* **29**: 192–201.

**Xiao Y, Zhu X-G. 2017.** Components of mesophyll resistance and their environmental responses: a theoretical modelling analysis. *Plant, Cell & Environment* **40**: 2729–2742.

**Xie K, Lu Z, Pan Y, Gao L, Hu P, Wang M, Guo S. 2020.** Leaf photosynthesis is mediated by the coordination of nitrogen and potassium: the importance of anatomical-determined mesophyll conductance to $CO_2$ and carboxylation capacity. *Plant Science* **290**: 110267.

**Xiong D, Flexas J. 2018.** Leaf economics spectrum in rice: leaf anatomical, biochemical, and physiological trait trade-offs. *Journal of Experimental Botany* **69**: 5599–5609.

**Xiong D, Flexas J. 2021.** Leaf anatomical characteristics are less important than leaf biochemical properties in determining photosynthesis responses to nitrogen top-dressing. *Journal of Experimental Botany* **72**: 5709–5720.

**Xiong D, Flexas J, Yu T, Peng S, Huang J. 2017.** Leaf anatomy mediates coordination of leaf hydraulic conductance and mesophyll conductance to $CO_2$ in *Oryza*. *New Phytologist* **213**: 572–583.

**Xu F, Wang K, Yuan W, Xu W, Shuang L, Kronzucker HJ, Chen G, Miao R, Zhang M, Ding M *et al.* 2019.** Overexpression of rice aquaporin OsPIP1;2 improves yield by enhancing mesophyll $CO_2$ conductance and phloem sucrose transport. *Journal of Experimental Botany* **70**: 671–681.

**Yamori W, Nagai T, Makino A. 2011.** The rate-limiting step for $CO_2$ assimilation at different temperatures is influenced by the leaf nitrogen content in several $C_3$ crop species. *Plant, Cell & Environment* **34**: 764–777.

**Zhu K, Wang A, Wu J, Yuan F, Guan D, Jin C, Zhang Y, Gong C. 2020.** Effects of nitrogen additions on mesophyll and stomatal conductance in Manchurian ash and Mongolian oak. *Scientific Reports* **10**: 1–10.

## Supporting Information

Additional Supporting Information may be found online in the Supporting Information section at the end of the article.

**Fig. S1** Number of studies per year and measurement methods applied to determine $g_m$.

**Fig. S2** Violin plots of $g_{m,25}$ for different PFTs by measurement method.

**Fig. S3** Violin plots of $g_{m,25}$ for crop species with at least five individual measurements.

**Fig. S4** Relationships between $g_{m,25}$ and leaf structural traits.

**Fig. S5** Relationships between $g_{m,25}$ and leaf anatomical traits.

**Table S1** Overview of leaf-level traits reported in this study.

**Table S2** Statistics of the main results in this study with $g_m$ standardised by two different temperature response functions.

Please note: Wiley Blackwell are not responsible for the content or functionality of any Supporting Information supplied by the authors. Any queries (other than missing material) should be directed to the *New Phytologist* Central Office.